ISSN 2093-8551
Vol. 1, No. 1, 2010, 25-30
DOI:10.5229/JECST.2010.1.1.025

Journal of Electrochemical Science and Technology

Composite Materials with MWCNTs and Conducting Polymer Nanorods and their Application as Supercapacitors

Lichun Liu[a], Sang-Hoon Yoo[b] and Sungho Park[c,†]
[a]*Department of Chemistry*
[b]*Department of Energy Science*
[c]*SKKU Advanced Institute of Nanotechnology, Sungkyunkwan University Suwon 440-746, South Korea*

ABSTRACT :

This study demonstrated the synthesis of high-surface-area metal-free carbonaceous electrodes (CE) from anodic aluminum oxide (AAO) templates, and their application as supercapacitors. Multi-walled Carbon nanotubes (MWCNTs) were interwoven into a porous network sheet that was attached to one side of AAO template through a vacuum filtration of the homogeneously dispersed MWCNT toluene solution. Subsequently, the conducting polymer was electrochemically grown into the porous MWCNT network and nanochannels of AAO, leading to the formation of a carbonaceous metal-free film electrode with a high surface area in the given geometrical surface area. Typical conducting polymers such as polypyrrole (PPY) and poly(3,4-ethylenedioxythiophene) (PEDOT) were examined as model systems, and the resulting electrodes were investigated as supercapacitors (SCs). These SCs exhibited stable, high capacitances, with values as high as 554 F/g, 1.08 F/cm^2 for PPY and 237 F/g, 0.98 F/cm^2 for PEDOT, that were normalized by both the mass and geometric area.

Keywords : AAO, MWCNT, Polypyrrole, PEDOT, Conducting polymer, Nanorods, Supercapacitor.

Received August 26, 2010 : *Accepted September 28, 2010*

1. Introduction

Carbonaceous electrodes are an important class of non-metal electrodes that have distinct chemical and physical properties, such as their native biocompatibility, wide potential window, low weight and cost, compared to metal electrodes.[1)] Apart from the original elementary carbon substances, a number of carbonaceous electrodes, especially polymers, with distinct chemical functional groups on their surfaces have been investigated in the fields of electrocatalysis,[2,3)] energy storage,[4,5)] sensing,[6-9)] and electronic devices.[10-12)] For example, according to a contribution from S. Patra and coworkers, a PEDOT film bearing electrochemically deposited platinum nanoparticles can enhance the electrocatalytic activity for the methanol oxidation in a direct methanol fuel cell (DMFC).[2)] K.S. Park et al.[4] incorporated $LiFePO_4$ into PPY as composite cathodes for lithium secondary baterries in order to increase the specific capacity and the rate capability and lower the overpotential at high discharge rates. A progress article discussed the conductivity and the work funtion parameters of the conducting polymer on a variety of topics, including chemiresitors, chemically sensitive FETs, capacitors and diodes[13]. Carbonaceous polymer electrodes are compatible to biomolecules, and the molecules of interest can be monitored and analyzed in biological matrixes, even in vivo. These significant applications are attributed to the good conductivity, redox states tunability, resonance-stabilized electronic structure and versatile functional group sites of the carbonaceous polymers. In general, an electrode with a larger surface area is crucial for practical applications in order to promote the electrode kinetics by increasing the interfacial area between the electrolyte and the electrode.

†Corresponding author. Tel.: +82-31-299-4562
E-mail address: spark72@skku.edu

To the best of our knowledge, the synthesis of a rod-like nanostructure using hard templates depends on the thermal evaporator and the elemental metals that are used to construct the electronic conducting layer. These elemental metals are expensive and cannot be used for the fabrication of metal-free carbonaceous products.[14-20] The preparation of a nonmetal conducting layer on AAO is very challenging. This study proposed a strategy to form an interconnected porous carbon nanotube network as the conducting layer in order to bypass the dependence of metallic conducting layers. This strategy took advantage of the filtration function of AAO under vacuum, and the carbonaceous material was on-pot electrodeposited into the MWCNT network and nanochannels of AAO in order to grow the vertical nanorods. This method specifically synthesized the carbonaceous film electrodes with a high surface area in a robust, facile, and inexpensive fashion.

Low-cost, mechanically flexible, and carbonaceous conducting polymers have been suggested as an ideal platform for highly capacitive SCs.[21] The newly devised carbonaceous electrode structures were exemplified SCs because of the fast reversible redox reaction of the conducting polymers and the electric double layer, along with the surface of the polymer materials.

2. Experimental

2.1. Materials

All of the chemicals were purchased from Sigma-Aldrich. The supporting electrolytes were prepared using double distilled H_2SO_4 with triple distilled Millipore MilliQ water ($\rho > 18.2$ MΩ·cm). The anodic aluminum oxide templates (diameter ≈ 25 mm, pore size ≈ 200 nm, thickness ≈ 60 mm) were purchased from Whatman International. The multi-wall carbon nanotubes (MWCNTs, CM-95) were purchased from Iljin, Korea.

2.2 Apparatus

The electrochemical depositions and measurements were performed using an Autolab ATU12 that was equipped with a three-compartment electrochemical Teflon cell. The anodic aluminum oxide templates with the conductive MWCNT film were placed on a sheet of ITO glass, which was used as the working electrode. Pt mesh and Ag/AgCl (3 M KCl) electrodes were employed as the counter and reference electrodes, respectively. The scanning electron microscope (SEM) images were acquired using a JEOL JSM-7401F field emission scanning electron microscope.

2.3. Preparation of carbonaceous electrodes

A mixture of 2.0 mg MWCNTs and 100 mL anhydrous toluene was ultrasonically dispersed in an airtight glass bottle for three hours until the solution was homogeneous. Then 20 mL of the prepared MWCNT solution was filtered through the AAO membrane for ten minutes with the aid of a conventional vacuum filtration pump. The resulting AAO template contained a MWCNT porous network coating on one side and was dried in an oven at 80ºC for 20 minutes in order to remove any toluene residue. Then, the ITO glass, with the AAO template and an insulating sealing O-ring, was used as the working electrode in a Teflon cell assembly like the one that Liu described.[22] After the acetonitrile electrolyte solutions (0.1 M monomer and 0.1 M $LiClO_4$[10,12,23]) were feed into a container in the Teflon cell, polypyrrole (PPY) and poly(3,4-ethylenedioxythiophene) (PEDOT) were potentiostatically grown into the prepared template at 1.2 V and 1.3 V (versus Ag/AgCl), respectively. After the polymerization, the polymer-filled AAO was rinsed with distilled water and subsequently immersed into 1 mL of a 3 M NaOH solution for 20 min in order to dissolve the AAO template in situ. After the AAO dissolution and repeated DI water rinsing, the carbonaceous electrodes with the nanorod array surfaces were completely developed. The polymer was also deposited on ITO glass without AAO template under the aforementioned conditions in order to prepare the non-nanorod polymer electrodes.

3. Results and Discussion

3.1. Carbonaceous electrodes

The synthesis process for the large-surface-area carbonaceous electrode is illustrated in Fig. 1. Typically, a thin MWCNT layer (~2 m) was constructed on one side of the AAO template through vacuum filtration with 20 mL of a MWCNT-toluene solution. Both the volume of the MWCNT solution and the filtration time were used to control the thickness of the MWCNT porous network layer, which determined the ultimate thickness of the composite bed in the final product. Figs. 1B and 1C show the MWCNT network on one side of the AAO template and a zoomed image of the MWCNT layer for the interwoven MWCNT network, respectively. The conducting polymers were electrochemically polymerized into MWCNT network because of the high conductivity and homogeneous compatibility of the MWCNTs with the polymers. When an electric potential was applied to the prepared composite template within the electrolyte, the

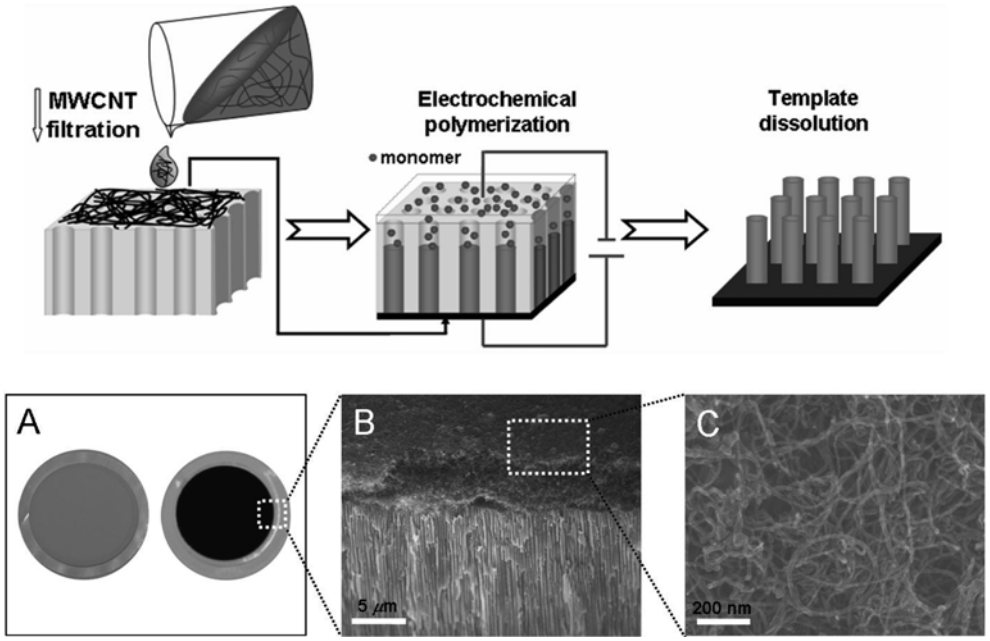

Fig. 1. Schematic illustration of fabrication process of large-surface-area carbonaceous film electrodes by the aid of MWCNTs network and AAO template (top panel). The optical photographs in A display the original AAO template (Left) and as-prepared AAO template (Right) after assembling a MWCNT conductive layer. SEM images B and C present composite product and local zoom-in morphology of MWCNT layer, respectively.

polymer initially grew into the MWCNT network. After the polymer was fully inserted into the voids of the MWCNT network, the polymer sequentially grew along the nano-channels of AAO, until the electric potential supply was terminated. In Fig. 2, the SEM images were obtained in order to observe the morphology of the product. Macroscopically, the nanorods exhibited locally aggregated domains, which were induced by the solvent evaporation during the sampling. In the bottom layer, the MWCNTs formed a skeleton, and the polymers filled in the gaps, as observed in the lower right inset images of Fig. 2. Notably, the contact between the polymer and the MWCNTs was solid because of the integrative structure of the two materials.

3.2. Supercapacitor application

The conducting polymers stored and released energy through anion doping/dedoping under electrical fields. The redox-type supercapacitor that was comprised of the conducting polymers provided a high power density, while maintaining the high specific capacitance. This can only occur if the slow ion-transport process during the polymer redox reaction is overcome by modifying the overall structure into a nanopillared or nanotubular structure.[7,10] The nanorods-decorated carbonaceous film electrodes were utilized as supercapacitors in order to evaluate their specific capacitance magnitudes, charge and discharge capabilities, as well as to compare their properties to the non-nanorod film electrodes. The active carbonaceous polymer films simultaneously served as the electrodes and the current collectors of the supercapacitors. The capacitive properties of the polymers (PPY was plotted with a solid line, and PEDOT was plotted with dashed lines) were characterized using cyclic voltammetry (CV) for the products with 0.5 M H_2SO_4 as the electrolyte (Fig. 3A). The pseudo-capacitance behavior was supported by the iterative diffusion of the counter anions (SO_4^{2-}) to and from the polymer matrix during the redox processes. The double-layer charging current was evident within the scanned electrical potential window. Generally, the capacitive energy is obtained from the discharge process, and the performance is monitored using the charge-discharge curves at a constant current under an appropriate potential window range. At a galvanostatic current of 5 mA/cm^2, the symmetric charge/discharge curves (Fig. 3B) of the SCs were obtained between –0.2 V and 0.6 V for PPY and between –0.4 V and 0.8 V for PEDOT. The cyclic abilities of the

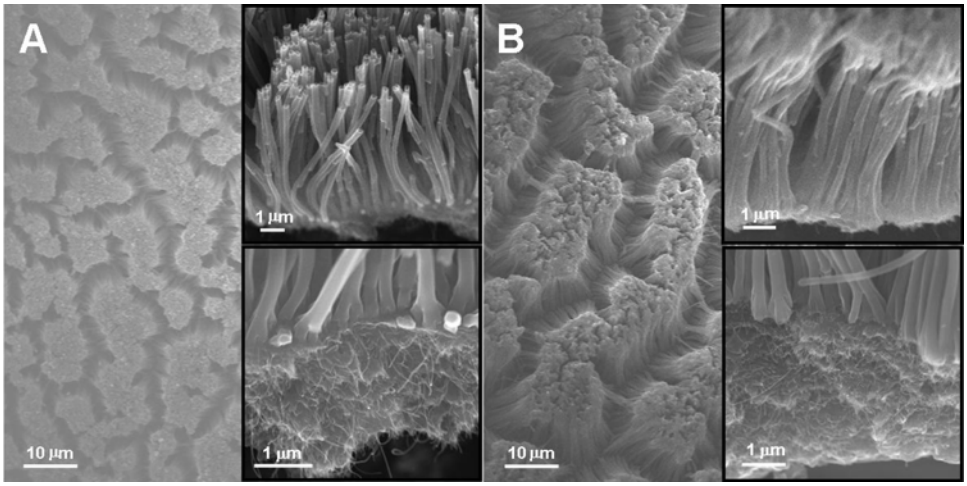

Fig. 2. Field-emission SEM images of PPY nanorod-surfaced film electrode (A) and PEDOT film electrode (B) with presence of full side contour view (upper right inset) and bottom layer close-up (lower right inset).

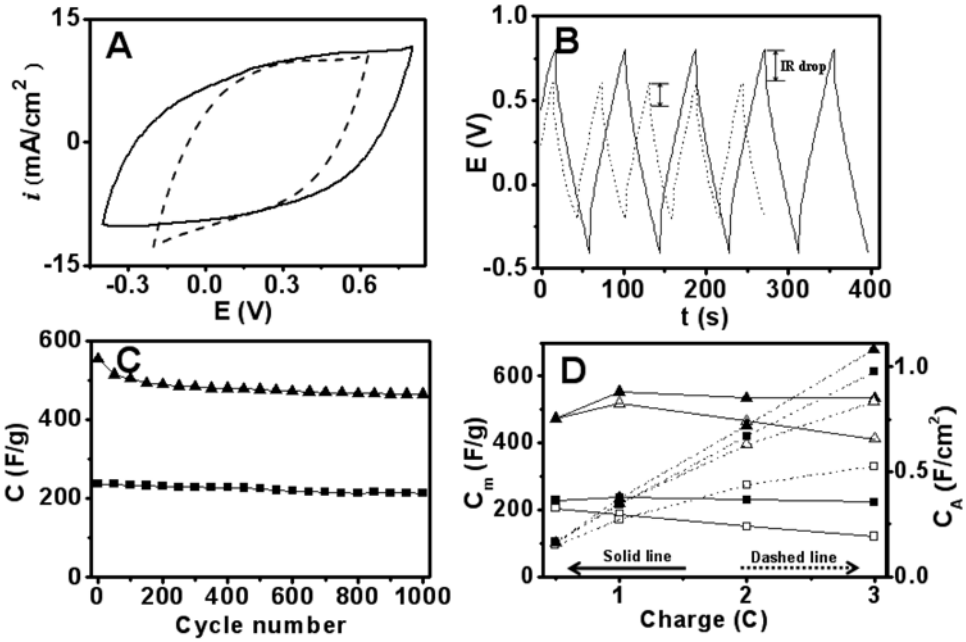

Fig. 3. A. Cyclic voltammograms of PPY (dotted line) and PEDOT (solid line) electrode. **B.** Galvanostatic charge-discharge curves of PEDOT nanorods film (solid line) between −0.4 V and 0.8 V and PPY nanorods film (dashed line) between −0.2 V and 0.6 V. **C.** The mass specific capacitance variations within 1000 cycles for PPY (▲) and PEDOT (■). **D.** Comparisons of mass specific capacitances and area specific capacitances between non-nanorod film electrodes (PPY, ▲; PEDOT, ■) and nanorod-surfaced film electrodes (PPY, △; PEDOT, □.) at various amount of charge passed. Dashed lines correspond to area specific capacitances (right longitudinal axis) and solid lines to mass specific capacitances (left). All electrochemical data were acquired using 0.5 M H_2SO_4 as electrolyte, scan rate at 50 mV/s, charge-discharge test at a current density of 5 mA/cm^2, 0.5 cm^2 geometric area of electrode in all experiments, and 1 C charge passed through polymerization (except D).

proposed SCs were evaluated for 1000 sample cycles of the charge-discharge process (Fig. 3C). The mass-specific capacitances (C_m) were calculated from the galvanostatic discharge curves using the following equation.[12, 24, 25)]

$$C_m(F/g) = \frac{J\Delta t}{m\Delta V} \quad \text{(Eq. 1)}$$

In this equation, J represents the current that was applied for the charge/discharge, Δt is the time that elapsed during the discharge cycle, m is the mass of the active electrode, and ΔV denotes the potential range of the discharge. In Fig. 3D, the subscript m was replaced with A, which denotes the geometric area in cm^2 in order to calculate the area-specific capacitance (C_A). In Fig. 3C, the mass-specific capacitance of PPY was visually much higher than PEDOT because of the lower mass of PPY. The specific capacitances of the non-nanorod film electrode and the fabricated nanorod film electrode that were prepared at 0.5, 1, 2, and 3 coulombs (C) are plotted in Fig. 3D for a systematic comparison. The mass-specific capacitance values of the PPY and PEDOT non-nanorod polymeric film electrodes dramatically decreased when additional polymers were formed on the identical geometric area. Therefore, the thicker films exhibited a higher resistance, suppressing the current density at a certain constant potential. Additionally, the restricted redox reaction occurred only on the adjacent surfaces and not deep inside of the electrode, where the polymers acted as a conductor with no contribution to the capacitance harvest. Likewise, similar results were also obtained by Fan[26] et al., who observed sharp decreases in the mass specific capacitances when the mass of deposited PPY film was over 0.6 mg/cm^2 for their method. In sharp contrast, in this study, the area specific capacitances (Fig. 3D) of the nanorod-surfaced film electrode demonstrated a significant linear increase ($R^2 = 0.999$) even at mass loadings of up to 2.0 mg/cm^2 (PPY) and 4.4 mg/cm^2 (PEDOT). Therefore, the composite film electrodes were effectively charged and discharged during operation because of the easy accessibility of the counter anions to the polymer matrix, resulting from the larger surface area, the effective thinness of the composite bed and the nanorod diameter, and the enhanced conductivity of the MWCNT network skeletal polymer bed. Consequently, the C_A values of the PPY (2.0 mg/cm^2) and PEDOT (4.4 mg/cm^2) nanorod arrays improved by 29% (1.08 : 0.84 F/cm^2) and 85% (0.98 : 0.53 F/cm^2), respectively, compared to the non-nanorod film electrodes. The capacitance harvest could be further enhanced using fabrication techniques for thicker templates in order to make more lengthy nanorods available.

The power and energy densities are essential parameters for evaluating the performances of the SCs in practical applications. Assuming an ideal SC, the energy density (E_d) and the power density (P_d) were calculated using the following equations.

$$E_d = \frac{1}{2}C_m U, \qquad P_d = \frac{E_d}{\Delta t} \quad \text{(Eq. 2, 3)}$$

In this equation, C_m is the mass-specific capacitance, U is the applied potential range during the charge-discharge process, and Δt represents the time during the discharge.

From Equations 1 and 2, the E_d values for the non-nanorod film electrodes decreased with increasing mass of the deposited in a given geometric area because the C_m values decreased (Figure 3D) for the non-nanorod surface. However, the films with the nanorods array surface, maintained constant C_m values, leading to high, stable E_d values. The internal resistance (R) was one of factors that influenced the SC performance and was also evaluated from the voltage drop at the start of each discharge stage (indicated by the arrows in Fig. 3B). The polymer nanorod and non-nanorod films exhibited different Rs. Typically, the non-nanorod films and proposed nanorod films that were prepared at 3C for exhibited R values of 75 and 62 Ω/□ for PPY and 110 and 60 Ω/□ for PEDOT, respectively. The R of the proposed film electrodes was evidently much lower than the non-nanorod film electrodes for both polymers. The E_d and P_d values of the proposed carbonaceous electrodes were superior to the non-nanorod electrodes because of the stable C_m and lower R values. The E_d (47 and 21 Wh/kg) and P_d (1950 and 630 W/kg) of the carbonaceous PPY and PEDOT nanorod-surfaced electrodes were high for polymeric SCs.

4. Conclusions

This study introduced showed that large-surface-area metal-free carbonaceous electrodes were readily fabricated with MWCNT networks and AAO templates without the involvement of any thermal apparatus or elemental metals. The interlaced MWCNT networks demonstrated a large effective surface area for the carbonaceous electrode for a given geometric area. The resulting carbonaceous polymer electrodes were exemplified the necessary properties for relevant supercapacitor applications. Additionally, the applications for the carbonaceous electrodes are not limited to the present context, and these proposed carbonaceous electrodes could positively impact a number applications, including electrocatalysis, sensing, energy storage, and electronic devices.

Acknowledgement

This work was supported by the National Research Foundation of Korea (World Class University (WCU): R31-2008-10029, Nano R&D program: 2010- 0019149, 2010-0015457, and Priority Research Centers Program: NRF-2009009 4025).

Reference

1. R.L. McCreery, *Chem. Rev.*, **108**, 2646 (2008).
2. S. Patra and N. Munichandraiah, *Langmuir*, **25**, 1732 (2008).
3. B. Rajesh, K.R. Thampi, J.M. Bonard, H.J. Mathieu, N. Xanthopoulos, and B. Viswanathan, *Chem. Commun.*, **16**, 2022 (2003).
4. K.-S. Park, S.B. Schougaard, and J.B. Goodenough, *Adv. Mater.*, **19**, 848 (2007).
5. Y.-H. Huang and J.B. Goodenough, *Chem. Mater.*, **20**, 7237 (2008).
6. S.A. Kumar and S.M. Chen, *Sensors*, **8**, 739 (2008).
7. Y. Cao, A.E. Kovalev, R. Xiao, J. Kim, T.S. Mayer, and T.E. Mallouk, *Nano Lett.*, **8**, 4653 (2008).
8. M. Ates and A.S. Sarac, *Prog. Org. Coat.*, **66**, 337 (2009).
9. H. Yoon and J. Jang, *Adv. Funct. Mater.*, **19**, 1567 (2009).
10. S.I. Cho, D.H. Choi, S.-H. Kim, and S.B. Lee, *Chem. Mater.*, **17**, 4564 (2005).
11. Y. Berdichevsky and Y.-H. Lo, *Adv. Mater.*, **18**, 1225 (2006).
12. S.I. Cho and S.B. Lee, *Acc. Chem. Res.*, **41**, 699 (2008).
13. J. Janata and M. Josowicz, *Nat. Mater.*, **2**, 19 (2003).
14. K.-B. Lee S. Park, and C.A. Mirkin, *Angew. Chem. Int. Edit.*, **43**, 3048 (2004).
15. H.-M. Bok, T.-Y. Shin, and S. Park, *Chem. Mater.*, **20**, 2247 (2008).
16. E.K. Payne, K.L. Shuford, S. Park, G.C. Schatz, and C.A. Mirkin, *J. Phys. Chem. B*, **110**, 2150 (2006).
17. S. Park, S.-W. Chung, and C.A. Mirkin, *J. Am. Chem. Soc.*, **126**, 11772 (2004).
18. H.-M. Bok, K.L. Shuford, S. Kim, S.K. Kim, and S. Park, *Nano Lett.*, **8**, 2265 (2008).
19. S. Kim, K.L. Shuford, H.-M. Bok, H.-M. Kim, and S. Park, *Nano Lett.*, **8**, 800 (2008).
20. S.-H.Yoo and S. Park, *Adv. Mater.*, **19**, 1612 (2007).
21. A.K. Shukla, S. Sampath, and K. Vijayamohanan, *Curr. Sci.*, **79**, 1656 (2000).
22. L.F. Liu, E. Pippel, R. Scholz, and U. Gosele, *Nano Lett.*, **9**, 4352 (2009).
23. R. Xiao, S.I. Cho, R. Liu, and S.B. Lee, *J. Am. Chem. Soc.*, **129**, 4483 (2007).
24. M. Kaempgen, C.K. Chan, J. Ma, Y. Cui, and G. Gruner, *Nano Lett.*, **9**, 1872 (2009).
25. J. Rajeswari, P.S. Kishore, B. Viswanathan, and T.K. Varadarajan, *Electrochem. Commun.*, **11**, 5725 (2009).
26. L.-Z. Fan and J. Maier, *Electrochem. Commun.*, **8**, 937 (2006).